Atmos. Meas. Tech. Discuss., https://doi.org/10.5194/amt-2018-224
Manuscript under review for journal Atmos. Meas. Tech.
Discussion started: 5 October 2018

Atmospheric Measurement Techniques
Discussions

The Fossil Fuel Emissions of Tokyo estimated directly from measurements of the Tsukuba TCCON site

Arne Babenhauserheide[1,*], Frank Hase[1], and Isamu Morino[2]

[1]IMK-ASF, Karlsruhe Institute of Technology (KIT), Karlsruhe, Germany
[2]National Institute for Environmental Studies (NIES), Tsukuba, Japan
[*]now at Disy Informationssysteme GmbH, Karlsruhe, Germany

Correspondence to: Arne Babenhauserheide (arne_bab@web.de)

Abstract. We present a simple approach for estimating the greenhouse gas emissions of large cities using accurate long-term data of column-averaged greenhouse gas abundances collected by a nearby FTIR (Fourier Transform InfraRed) spectrometer.

We estimate the average yearly carbon emissions from the area of Tokyo to be $86 \pm 33 \frac{MtC}{\mathrm{year}}$ between 2011 and 2016, calculated using only measurements from the TCCON site in Tsukuba (north-east of Tokyo) and wind-speed data from nearby radiosondes.

1 Introduction

Anthropogenic emissions of carbon dioxide are the strongest long-term control on global climate (Collins et al., 2013, Figure 12.3, page 1046), and the Paris agreement (secretariat, 2015) "recognizes the important role of providing incentives for emission reduction activities, including tools such as domestic policies and carbon pricing". Implementing carbon pricing policies as an effective tool to reduce emissions and stimulate research requires accurate measurements of carbon emissions (Kunreuther et al., 2014, ch. 2.6.4 and 2.6.5, pp. 181ff).

The carbon dioxide footprint of large scale fossil fuel burning emitters has been retrieved from satellite (Bovensmann et al., 2010; Hakkarainen et al., 2016; Hammerling et al., 2012; Hakkarainen et al., 2016; Ichii et al., 2017; Deng et al., 2014; Butz et al., 2016) and via ground based differential measurements using multiple mobile total column instruments (Frey et al., 2015; Hase et al., 2015; Chen et al., 2016). Inverse modelling allows coupling in-situ measurements (which only capture enhancements in mixing ratio close to the ground) with atmospheric transport for similar investigations (i.e. van der Laan-Luijkx et al., 2017; Basu et al., 2011; Babenhauserheide et al., 2015; van der Velde et al., 2014b; Meesters et al., 2012), but due to short mission times of satellites and differential measurement campaigns and high uncertainties when using in-situ data, long term changes in emissions are typically derived from economic fossil fuel and energy consumption data (i.e. Andres et al., 2011; Bureau of the Environment Tokyo, 2010; Peters and van der Laan-Luijkx, 2012; van der Velde et al., 2014a; Le Quéré et al., 2015, 2016).

The Total Carbon Column Observing Network (TCCON, Wunch et al., 2011; Toon et al., 2009) provides highly accurate and precise total column measurements of carbon dioxide mixing ratios with multi-year records of consistently derived data.

The aim of our study is to provide an estimate of the Tokyo CO_2 emissions by correlating measured XCO_2 with wind speed and direction, resulting in a measurement-driven approach to derive the annual carbon dioxide emissions of Tokyo city (Japan) using four years of measurements (2011-08-04 – 2016-03-30) by the TCCON site at Tsukuba, Japan, along with radiosonde measurements of daily local wind profiles. This method provides an inexpensive approach to estimate city emissions which is easy to reproduce and to establish, and is suitable for long-term monitoring.

2 Observations

The column data from TCCON provides the currently best measurements of the column averaged CO_2 abundances. The average station-to-station bias is less than 0.2 ppm (Wunch et al., 2011).

The stations of the TCCON-network measure the absorption of CO_2 in the solar spectrum (Wunch et al., 2011). Dividing this absorption by the absorption of O_2 yields a pressure-independent measure for the concentration of carbon dioxide in the atmospheric column (XCO_2). The precision of these measurements is better than 0.2ppm (0.2%) by Messerschmidt et al. (2011). Since this study restricts itself to a single station it can ignore constant scaling factors.

This study uses the current dataset of column-averaged carbon dioxide abundances generated with GGG2014 from solar absorption spectra recorded at the Tsukuba TCCON station, Japan (Ohyama et al., 2009; Morino et al., 2016). Publicly available data from Tsukuba at the TCCON data site[1] used in this study extends from 2011-08-04 to 2016-03-30. The coordinates of the Tsukuba TCCON site are 140.12° East and 36.05° North, the altitude is 31m. Essential information about the TCCON site in Tsukuba is available from the TCCON wiki [2] In addition to concentration data of trace gases, the station provides wind direction and speed measured at the rooftop of the observatory.

[1]TCCON data is publicly available from tccondata.org
[2]The TCCON wiki is located at https://tccon-wiki.caltech.edu/Sites/Tsukuba

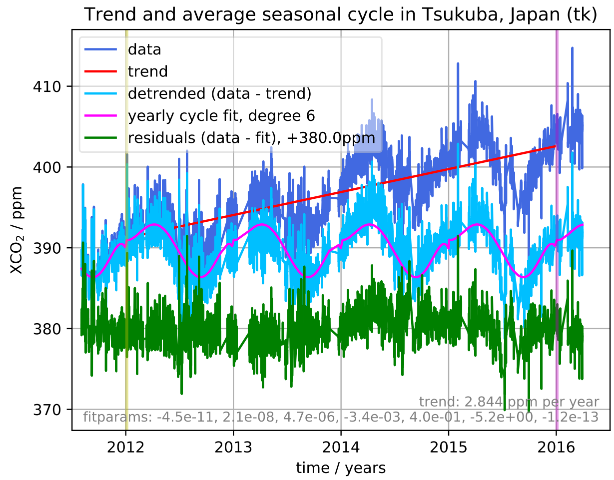

Figure 1. Detrending and deseasonalization of the XCO_2 total column measurements in Tsukuba, Japan. The trend (shown as a red "trend" line) is removed with a linear least squares fit to the data from background directions between 2012-01-01 and 2016-01-01 (denoted by the yellow and magenta vertical lines), the seasonal cycle from the signal due to photosynthesis, respiration and decay (shown as "yearly cycle fit, degree 6") is removed by fitting a polynomial of degree 6 to the combined yearly cycles of the detrended data. Degree 6 was chosen empirically.

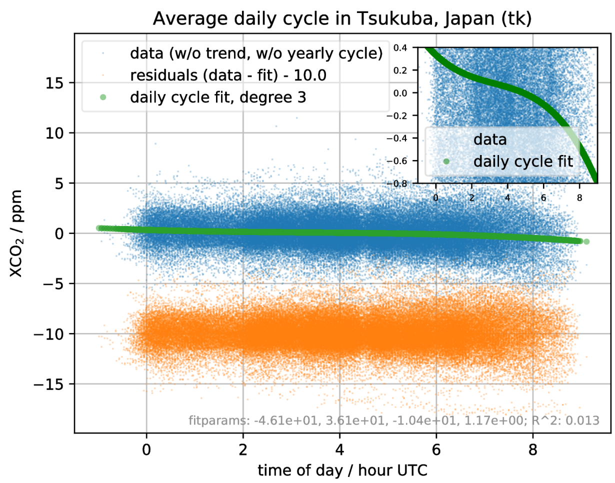

Figure 2. To remove a potential bias from correlation of wind direction and daytime which would couple the signal from photosynthesis and respiration, the daily cycle is removed by fitting and subtracting a polynomial of degree 4. Degree 4 was chosen empirically.

Atmospheric Measurement Techniques Discussions

3 Removing trend and natural cycles

To estimate the emissions of Tokyo directly from the measurements, they must be made accessible to a simple statistical analysis. Column averaged atmospheric CO_2 abundances are subject to strong seasonal variations and a yearly rise of about 2.0 ppm per year (Hartmann et al., 2013, page 167 in section 2.2.1.1.1). Additionally there's an average daily cycle of about 0.3 ppm in the densely measured daytime between 2:00 UTC and 7:00 UTC (local time between 11:00 and 16:00 GMT+9). To allow direct comparisons of values from different times of year and times of day, these cycles are removed by fitting and subtracting polynomials from the data: linear for the trend, degree 6 for the yearly cycle (roughly equivalent to bi-monthly granularity) and degree 3 (roughly 3-hour granularity) for the daily cycle. The trend is fitted against measurements from background directions, but the daily cycle is fitted against measurements from all directions, so the fitting might remove a certain amount of the actual daily cycle of emissions. However the impact of this fitting in final estimates is limited to wind directions correlated with the time of day. Such a correlation exists, but mainly outside the densely measured daytime (a graph is available in the supplement of this paper). The programs are provided in the supplement of this paper. Figure 1 and 2 show the fits and residuals from the process. The calculations only use data provided directly from the TCCON network. The degrees of the fits were chosen empirically (by manual adjustment) to minimize the residuals over all TCCON sites available in 2016.

Atmos. Meas. Tech. Discuss., https://doi.org/10.5194/amt-2018-224
Manuscript under review for journal Atmos. Meas. Tech.
Discussion started: 5 October 2018

Atmospheric Measurement Techniques
Open Access
Discussions

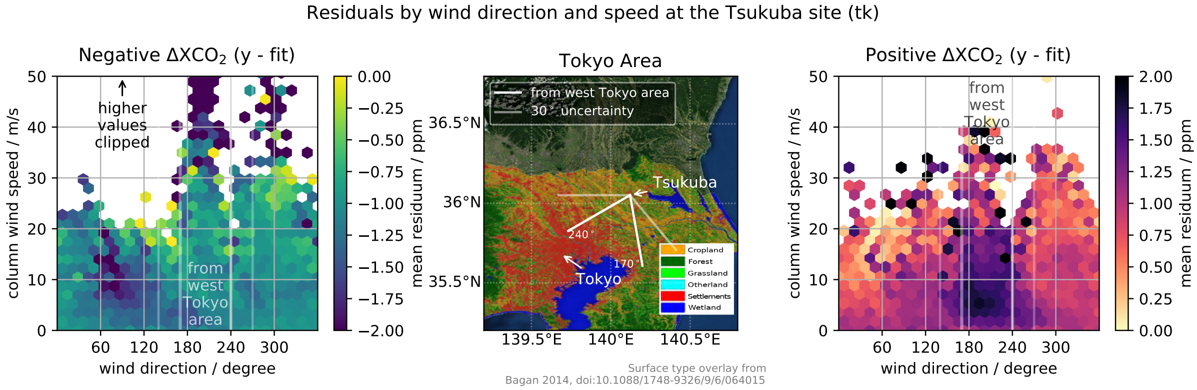

Figure 3. The **center graph** shows a map of Tokyo and its surroundings, retrieved from the ArcGIS REST service[3] with an overlay indicating the surface type. The colors in the overlay visualize land-use and settlement density (taken from Bagan and Yamagata, 2014). It clearly shows decreasing population density with distance from Tokyo city, along with the long tail of Tokyo settlements towards the north west. Close by Tokyo Bay in the lower center of the map, at the south east perimeter of Tokyo and on the opposite shore, there are multiple coal and gas power plants. Tokyo city center and the position of the TCCON site in Tsukuba are marked along with white lines which form an opening angle for incoming wind at Tsukuba which is interpreted as coming from Tokyo Area, along with additional widening by 30° as estimate of the actual origin of transported CO_2 arriving at Tsukuba from the given wind direction. These white lines denoting the incoming wind angle limits are reproduced in the **right graph** and the **left graph** as delimiting directions in which the wind blows from west Tokyo area. The **right** graph shows the **positive** half of the residuals from Figure 2, binned by wind direction and -strength. The color represents the mean value of the positive residuals within the bin. The **left** graph shows the **negative** half of the residuals from Figure 2, binned by wind direction and -strength. The color represents the mean value of the negative residuals within the bin. The black arrow at the upper edge of the left graph indicates that values for wind speeds above 50 m/s have been left out to focus on the area between 5 and 15 m/s used in the later evaluation. Splitting the residuals into positive and negative values is done to simplify visual detection of emissions without interference from effective sinks. In the following, detailed treatment of the residuals uses both positive and negative residuals.

4 Directional dependence of remaining differences

To calculate the carbon source of Tokyo, the residuals described in section 3 are binned by wind direction and speed, as shown in Figure 3. A major source of uncertainty in this endeavor is the actual extent of Tokyo. This extent was chosen as 170° to 240° as seen from the TCCON site in Tsukuba, following the 2D histogram shown in the right panel in Figure 3. Within these directional delimiters, the interval with wind speeds between 5 and 15 ms^{-1} contains only bins with an enhanced concentration of CO_2. Perfect definition of these limits isn't possible in the Scheme presented here, because the area can only be delimited orthogonal to the wind direction measured in Tsukuba. In parallel direction the only limit are changes in wind direction over time. This is indicated by the weaker enhancement seen for wind speeds below 5 ms^{-1}.

[3]retrieved as EPSG:4301 using a ESRI_Imagery_World_2D request to server.arcgisonline.com/ArcGIS via the basemap library in matplotlib (Hunter, 2007) as described at basemaptutorial.readthedocs.io/en/latest/backgrounds.html#arcgisimage. Used with permission (Permission for publication of this graph under creativecommons attribution license granted by Esri). Copyright (c) (2017) Esri, ArcGIS. All rights reserved.

Using ΔXCO_2, a measure proportional to the carbon dioxide column enhancement, and the effective wind speed ascribed to these enhancements from the direction of Tokyo allows estimating the source of Tokyo. However, the directly measured wind speed which is provided by the TCCON network only provides an approximate indication of the effective wind speed and direction in the altitude range carrying the enhanced carbon dioxide (similar to the effects discussed by Chen et al., 2016, for differential measurements of the emissions).

4.1 Effective wind speed

Estimating the wind speed of air with enhanced carbon dioxide concentrations due to emissions from Tokyo requires taking the difference in height of the measured concentrations and the measured wind speed into account. To this end, the ground wind speed v_{wind} can be replaced by the density weighted average wind speed profile within the boundary layer, as seen in trajectories from Tokyo, calculated with hysplit (Rolph et al., 2017; Stein et al., 2015). These trajectories show that most air parcels from Tokyo arriving at Tsukuba are contained within the lowest 2km of the atmosphere. Radiosonde data from Tateno, Japan, situated close to Tsukuba station, provides 7 years of measurements from 2009 to 2016. The data was retrieved from the Atmospheric Soundings site at University of Wyoming (http://weather.uwyo.edu/upperair/sounding.html). One example of these data sets is by Ijima (2016). Further details are available in the auxiliary material, provided as Babenhauserheide and Hase (2018).

Figure 4 visualizes the variability of the profile by atmospheric pressure. The average wind speed in the profile is used to derive daily scaling factors from the ground wind speed to the average profile wind speed. These scaling factors are applied to the ground wind speed measured at the TCCON site in Tsukuba to estimate the effective wind speed of the volume of air with enhanced carbon dioxide concentration in the total column.

These scaling factors are provided in the auxiliary material (Babenhauserheide and Hase, 2018) but provide a significant source of uncertainty, since their use rests on the assumption on uniform mixing of the carbon emissions across the boundary layer. Forward trajectory calculations with HYSPLIT (Stein et al., 2015) suggest that 50 km transport distance suffices for particles to reach the top of the boundary layer, but they do not prove that this suffices to generate a uniform CO_2 mixing ratio. Therefore, as also seen by Chen et al. (2016), the unknown actual transport pathway of emitted CO_2 to the measurement location is a significant source of uncertainty.

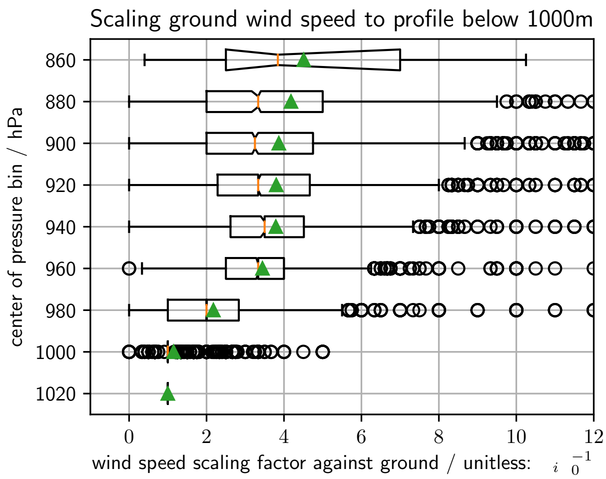

Figure 4. Wind speed profile statistics up to 1000 m at Tateno, Japan using data from 2009 to 2016, including Ijima (2016). Values are calculated by dividing the wind speed at a given pressure by the wind speed at the lowest level. The boxplots show the median (red line) and the mean (green triangle). 50% of values are within the box, the whiskers include 95% of the values and the rest is shown as outliers (black circles). The notch in the box shows the uncertainty of the median calculated via resampling.

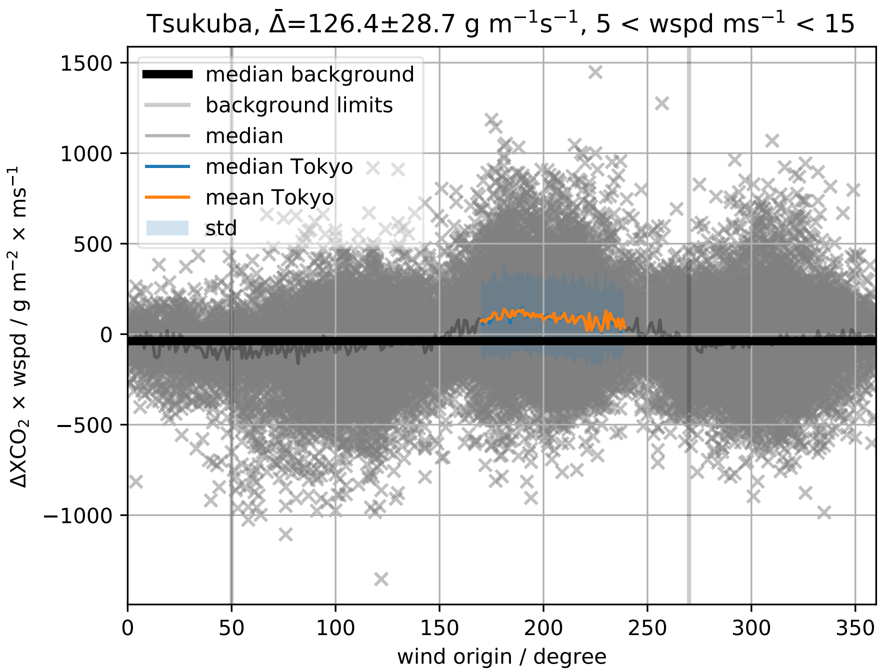

Figure 5. Residuals multiplied by wind speed plotted against the wind direction for scaled wind speeds between 5 ms^{-1} and 15 ms^{-1}; measured by the TCCON site in Tsukuba, Japan. The mean enhancement $\bar{\Delta}$, the mean Tokyo and median Tokyo and the std are calculated for the directions defined as from Tokyo in section 3. The median background is calculated from the residuals outside the background limits (drawn as vertical lines).

5 Estimated carbon source of Tokyo

To calculate the source of Tokyo S_T, the measured total column enhancement E_m (in $[g_{CO_2}]$) is multiplied with the *area affected per second* by the emission source from within Tokyo area, $A_{aff,Tokyo}$ (in $\left[\frac{m^2}{s}\right]$):

$$S_T = E_m \cdot A_{aff} \tag{1}$$

This affected area per second can be calculated from the wind speed of the volume of air with enhanced concentrations at the measurement location, approximately the average column wind speed v_{wind}, and the spread of the Tokyo area perpendicular to the wind speed $s_\perp$.

$$A_{aff} = v_{\text{wind}} \cdot s_\perp \tag{2}$$

The perpendicular spread $s_\perp$ is calculated by assuming that total columns of carbon dioxide from Tokyo area are transported to the measurement location without effective divergence perpendicular to the wind direction and assuming approximately

Atmos. Meas. Tech. Discuss., https://doi.org/10.5194/amt-2018-224
Manuscript under review for journal Atmos. Meas. Tech.
Discussion started: 5 October 2018

circular city structure. Therefore this spread can be approximated from the distance between Tokyo city center and the TCCON measurement site in Tsukuba:

$$s_\perp \approx 2\pi \cdot s_{\text{Tsukuba–Tokyo}} \cdot \frac{\Delta\alpha}{360°} \tag{3}$$

with $\Delta\alpha$ the opening angle of the limits of wind directions associated with Tokyo and $s_{\text{Tsukuba–Tokyo}} \approx 65$km. The city center of Tokyo was chosen to be at the palace. Due to measuring total columns, vertical divergence only affects the height of the enhancement in the column and therefore the wind speed of air with enhanced concentrations at the measurement location. Treating 170° to 240° as wind direction coming from Tokyo, this yields a perpendicular spread of 79.4 km.

The angle-integrated $E_m \Delta t_{aff}$ is collected into contributions from different wind directions as shown in equation 4:

$$E_m A_{aff} = \int\limits_\alpha E_{m,\alpha} A_{aff,\alpha} d\alpha = \frac{s_\perp}{\Delta\alpha} \cdot \int\limits_\alpha E_{m,\alpha} v_{\text{wind},\alpha} d\alpha = s_\perp \bar{\Delta}_{CO_2} \tag{4}$$

Here $\bar{\Delta}_{CO_2}$ denotes the mean enhancement as depicted in Figure 5.

$\bar{\Delta}_{CO_2}$ is calculated from the XCO_2 residuals. The residuals are calculated by subtracting the trend and fits to the yearly and daily cycle following equation 7 as described in section 3. To calculate $\bar{\Delta}_{CO_2}$, the median total column residual from background wind directions (chosen as 310° to 50°, using 0° as from north by meteorological conventions) is subtracted from the target direction residuals (see equation 8), then the result is multiplied with the wind speed during the time of measurement. Finally it is converted from measured total column concentration $C_{CO_2,t,\text{col}}$ to total column mass $m_{CO_2,\text{col}}$ using equations 5 and 6.

$$\text{unit air column mass:} \quad m_{\text{air,col}} = \frac{p_t}{g_{a_t,t}} \cdot 10^5 \left[\frac{g}{m^2}\right] \tag{5}$$

$$CO_2 \text{ column mass:} \quad m_{CO_2,\text{col}} = \frac{M_{CO_2}}{M_{\text{air}}} \frac{m_{\text{air,col}}}{f_{col}} \cdot C_{CO_2,t,\text{col}} \tag{6}$$

$$\text{total column residuum:} \quad R = m_{CO_2,\text{col}} - m_{CO_2,\text{col},\textbf{seasonal cycle fit}} - m_{CO_2,\text{col},\textbf{daily cycle fit}}; \text{(described in section 3)} \tag{7}$$

$$\text{enhancement:} \quad E_m = R_{\text{from Tokyo area}} - \text{median}\left(R_{\text{from background}}\right) \tag{8}$$

at time t, level l and daily apriori a_t[4] with

tracer mass	$m_{\text{gas,col}}$,
total column air mass	$m_{\text{air,col}}$,
column concentration	$C_{CO_2,t,\text{col}}$,
molar masses	$M_{CO_2} = 44.0 \frac{g}{mol}$ and $M_{\text{air}=28.9 \frac{g}{mol}}$,
gravity	$g_{a_t,l}$ (from TCCON apriori),
pressure	p_t.

[4] $f_{col} = 0.9975$ is a column mass correction following Bannon et al. (1997)

Atmos. Meas. Tech. Discuss., https://doi.org/10.5194/amt-2018-224
Manuscript under review for journal Atmos. Meas. Tech.
Discussion started: 5 October 2018

Atmospheric Measurement Techniques Discussions
Open Access

From the mean enhancement $\bar{\Delta}_{CO_2}$ the source of Tokyo is derived as

$$.S_T = \bar{\Delta}_{CO_2} \cdot s_\perp = 126 \pm 29 \frac{g_{CO_2}}{ms} \cdot 79400m = 10.0 \pm 2.3 \frac{t_{CO_2}}{s} \tag{9}$$

The given uncertainty is taken from the standard deviation as shown in Figure 5.

For comparison with city emission inventories, the CO_2 source is scaled to yearly carbon emissions:

$$\begin{aligned} S_{T,\mathrm{C,yearly}} &= \bar{\Delta}_{CO_2} \frac{M_C}{M_{CO_2}} s_\perp \cdot \frac{s}{\mathrm{year}} & (10)\\ &= 126 \pm 29 \left[\frac{g_{CO_2}}{ms}\right] \cdot \frac{12}{44} \left[\frac{g_C}{g_{CO_2}}\right] \cdot 79400m \cdot 31557600 \frac{s}{\mathrm{year}} & (11)\\ &= 86 \pm 20 \frac{Mt_C}{\mathrm{year}} & (12) \end{aligned}$$

For comparison with gridded emission inventories, the CO_2 emissions are scaled to average monthly carbon emissions per wind direction (in 1° steps):

$$\begin{aligned} S_{\tau,\mathrm{CO_2,average,deg,monthly}} &= \bar{\Delta}_{CO_2} \frac{M_C}{M_{CO_2}} s_\perp \cdot \frac{s}{\mathrm{month} \cdot \mathrm{degree}} & (13)\\ &= 126 \pm 29 \left[\frac{g_{CO_2}}{ms}\right] \cdot \frac{12}{44} \left[\frac{g_C}{g_{CO_2}}\right] \cdot 1134m \cdot 2592000 \frac{s}{\mathrm{month} \cdot \mathrm{degree}} & (14)\\ &= 101 \pm 23 \frac{kt_C}{\mathrm{month} \cdot \mathrm{degree}} & (15) \end{aligned}$$

Atmos. Meas. Tech. Discuss., https://doi.org/10.5194/amt-2018-224
Manuscript under review for journal Atmos. Meas. Tech.
Discussion started: 5 October 2018

Atmospheric Measurement Techniques Discussions

6 Estimating uncertainties

In addition to the statistical uncertainty and the uncertainty of the wind profile discussed in section 4.1, the estimated emission depends on the selected extent of Tokyo area and is limited by the unknown actual distribution ofd istances of emission sources from the measurement site at Tsukuba.

Choosing different opening angles for air *from Tokyo area* yields a yearly emission range from $54.0 \pm 7.4 MtC$year^{-1} when choosing air *from Tokyo area* between 180° and 220° up to $93 \pm 35 MtC$year^{-1} when choosing air *from Tokyo area* between 150° and 260°. This uncertainty also plays a role in comparisons, if the actual wind direction higher up in the atmosphere is not distributed symmetrically around the wind direction at ground.

The distance of emission sources from the TCCON site in Tsukuba affects the estimated spread of the emission region perpendicular to the wind direction. This calculation assumes symmetric distribution of emission strengths parallel to the wind direction. This assumption is plausible, since the most densely populated region of Tokyo extends to the north west towards the prefecture of Saitama. However Bagan and Yamagata (2014) and Oda and Maksyutov (2011) show a similar extension towards the south east, and the power plants are southward of the palace. If the "center of mass" of the emissions were located 10 km further away from the site, this would yield a 15% increase of the estimate, in absolute numbers $\pm 13 \frac{MtC}{\text{year}}$. This uncertainty always needs to be taken into account. Consequently the most robust estimate of the emissions of Tokyo is

$$\text{Yearly carbon emissions of Tokyo:} \quad S_{T,\text{C,yearly}} = 86 \pm 20 \pm 13 \frac{MtC}{\text{year}} \tag{16}$$

$$\text{Monthly carbon dioxide emissions of Tokyo:} \quad S_{\tau,\text{CO}_2,\text{average,deg,monthly}} = 101 \pm 23 \pm 15 \frac{ktC}{\text{month} \cdot \text{degree}} \tag{17}$$

These values provide an estimate of the source of Tokyo calculated directly from measurements. The measurements are only conducted in the hours of day between 0 UTC and 8 UTC, though, and the fossil fuel source of Tokyo might be different during nighttime due to reduced human activity. Nassar et al. (2013) provide hourly scaling factors for fluxes for global models. In the measurement interval these scaling factors are 1.09, 1.11, 1.13, 1.16, 1.16, 1.18, 1.20, 1.21 and 1.188 which gives an average factor of 1.16, with the standard deviation given as 0.15. Dividing the fluxes by 1.16 gives an estimate of the fluxes which would be derived from measurements around the day. This would result in a total emission estimate of $74 \pm 38 \frac{MtC}{\text{year}}$.

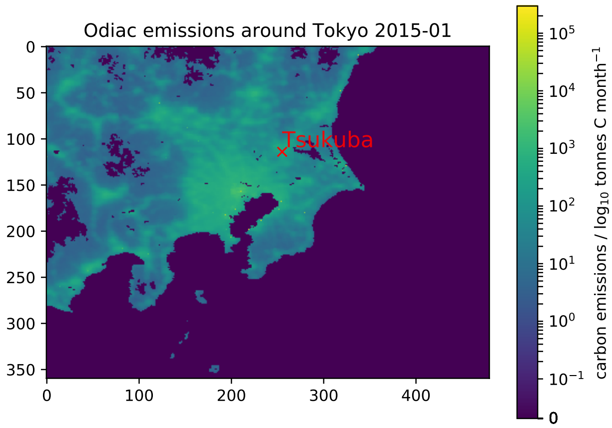

Figure 6. Odiac carbon emissions per 1km×1km in pixel for January 2015 in $\log_{10}$ scale. This graph is created directly from the 1km×1km Odiac dataset (Oda and Maksyutov, 2011) to visualize its structure.

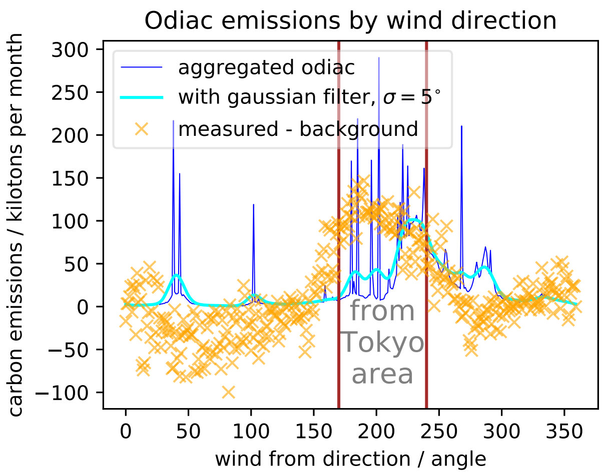

Figure 7. Sum of Odiac carbon emissions by direction as seen from Tsukuba, Japan. The “aggregated odiac” emissions show emissions per direction from beginning of 2011 to end 2016. The gaussian filter data uses a moving average with gaussian weight to estimate signals measured at a distance. The measured dataset shows the median residuals from figure 5 for comparison.

7 Comparison with other Datasets

To compare the results with the high-resolution Odiac emission inventory (Oda and Maksyutov, 2011),[5] using the regional slice shown in Figure 6. Measurements are simulated from Odiac by summing over all emissions *from Tokyo area* from 2011 to 2016 as (emissions by angle are shown in Figure 7), and then subtracting the sum of the emissions *from background directions*:

$$\frac{1}{5}\sum_{t=2011-01}^{2015-12}\left(\sum_{\alpha}^{\text{Tokyo}} E_{odiac,t,\alpha} - \sum_{\beta}^{\text{bg}} E_{odiac,t,\beta}\right) = 40.4\frac{MtC}{\text{year}}, \tag{18}$$

which is around half the emissions estimated in this paper from TCCON measurement data and within two standard deviations (2σ) of the estimated emissions. With the scaling for the time of day of the measurement, Odiac results lie within one standard deviation of the estimate in this paper.

The peak of the distribution of emissions (within "from Tokyo area") is shifted about 30° counterclockwise from model to measurements. This is within the expected shifts due to the typical shift in wind direction between measurements conducted close to the ground and measurements higher up in the planetary boundary layer. These discrepancies could be corrected for by using more complex atmospheric transport, but that would then require every reproduction to run such a transport, which would defeat the purpose of this study, namely to provide an easily reusable approach for estimating city emissions.

The economic data published by the Bureau of the Environment Tokyo (2010) report emissions of $57.7\frac{MtCO_2}{\text{year}}$ in the fiscal year 2006 for the Tokyo Metropolitan Area. This is equivalent to $15.7\frac{MtC}{\text{year}}$ and shows a larger discrepancy to our results. This discrepancy which likely stems from different definitions for the source area. Part of this discrepancy cannot be reconciled, because the method shown in this paper cannot limit the emission aggregation parallel to the wind direction.

[5] Odiac data retrieved from http://odiac.org

8 Conclusions and Outlook

We find that a single multi-year dataset of precise column measurements provides valuable insights into the carbon emissions of city-scale emitters. The estimated emissions of 86 ± 33 megatons carbon per year found for Tokyo has less than 40% uncertainty despite our intentionally chosen constraint to use only a basic evaluation scheme which can be repeated on any personal computer with publicly available data. While the operation of a TCCON station is a major effort, a decade of CO_2 column measurements of comparable quality can be conducted with affordable and easier to operate mobile spectrometers (see for example Frey et al., 2015) which opens an avenue for every country to measure and evaluate emissions of mega cities: Placing a single total column measurement site in the vicinity of a major city allows estimating its emissions. This can complement global source and sink estimates and improve acceptance of carbon trading programs by enabling independent verification of findings.

The uncertainties in these estimates could be reduced further by taking into account more detailed wind fields from meteorological models, by correcting for the wind direction at different altitudes and by correcting for the diurnal cycle of fossil fuel emissions. These corrections are already taken into account in source-sink estimates based on inverse modelling of atmospheric transport (i.e. van der Laan-Luijkx et al., 2017; Riddick et al., 2017; Massart et al., 2014; Basu et al., 2013), therefore we restrict ourselves to the simpler evaluation which allows us to stick closely to easily accessible data which keeps our findings easy to replicate.

Further uncertainty reductions can be achieved by establishing several observing sites within and around the source area. This approach also provides information about the spatial structure of emissions and can be used in focused measurement campaigns to obtain constraints for evaluation of measurements with lower spatial resolution as well as long term datasets. The provided yearly emission estimates could be improved by calculating the diurnal scaling of the emission source from CO_2 concentration measurements of an in-situ instrument.

To complete this outlook, we would like to suggest that the negative values seen on the left graph of Figure 3 at a wind direction around 60° indicate that it might also be possible to detect biospheric drawdown of CO_2 by woodland with just a single total column instrument.

We conclude that long-term ground-based measurements of column-averaged greenhouse gas abundances with sufficient accuracy for detecting the signals of local emission sources are a cost-efficient approach to improve our knowledge about sources and sinks of greenhouse gases.

Code and data availability. All code used and pre-processed data in JSON format (as described in RFC 7159) are available in the supplementary material. See the README in the supplementary material for usage information. The non-included data is publicly available from the TCCON data portal (tccondata.org), from the Odiac project odiac.org, and from the Atmospheric Soundings site at University of Wyoming (weather.uwyo.edu/upperair/sounding.html.

Competing interests. The authors have no competing financial interests, but they are working on other projects with ground-based total column measurement instruments.

Acknowledgements. Large parts of the inspiration for this method of evaluation and of the boldness to keep it simple are due to our treasured colleague Dr. Friedrich Klappenbach (especially his evaluation of CO_2 in Klappenbach et al., 2015) and the simple estimate of effective boundary layer wind speed from radiosonde data was suggested by Dr. Bernhard Vogel. Matthias Frey contributed insights into differential measurements of the Tokyo source using multiple portable spectrometers, as well as fruitful discussions about these evaluations. Support for this study was provided by the Bundesministerium für Bildung und Forschung (BMBF) through the ROMIC project, with funding for initial work provided by the Emmy-Noether program of the Deutsche Forschungsgemeinschaft (DFG) through grant BU2599/1-1 (RemoteC).

The article processing charges for this open-access publication have been covered by a Research Centre of the Helmholtz Association.

Atmospheric Measurement Techniques Discussions

References

Andres, R. J., Gregg, J. S., Losey, L., Marland, G., and Boden, T. A.: Monthly, global emissions of carbon dioxide from fossil fuel consumption, Tellus B: Chemical and Physical Meteorology, 63, 309–327, doi:10.1111/j.1600-0889.2011.00530.x, 2011.

Babenhauserheide, A. and Hase, F.: Code and Data for amt-2018-224, doi:10.5281/zenodo.1444068, 2018.

Babenhauserheide, A., Basu, S., Houweling, S., Peters, W., and Butz, A.: Comparing the CarbonTracker and TM5-4DVar data assimilation systems for CO_2 surface flux inversions, Atmospheric Chemistry and Physics, 15, 9747–9763, doi:10.5194/acp-15-9747-2015, http://www.atmos-chem-phys.net/15/9747/2015/, 2015.

Bagan, H. and Yamagata, Y.: Land-cover change analysis in 50 global cities by using a combination of Landsat data and analysis of grid cells, Environmental Research Letters, 9, 064 015, doi:10.1088/1748-9326/9/6/064015, http://stacks.iop.org/1748-9326/9/i=6/a=064015, 2014.

Bannon, P. R., Bishop, C. H., and Kerr, J. B.: Does the Surface Pressure Equal the Weight per Unit Area of a Hydrostatic Atmosphere?, Bulletin of the American Meteorological Society, 78, 2637–2642, doi:10.1175/1520-0477(1997)078<2637:dtspet>2.0.co;2, http://dx.doi.org/10.1175/1520-0477(1997)078<2637:DTSPET>2.0.CO;2, 1997.

Basu, S., Houweling, S., Peters, W., Sweeney, C., Machida, T., Maksyutov, S., Patra, P. K., Saito, R., Chevallier, F., Niwa, Y., Matsueda, H., and Sawa, Y.: The seasonal cycle amplitude of total column CO_2: Factors behind the model-observation mismatch, Journal of Geophysical Research: Atmospheres, 116, doi:10.1029/2011JD016124, 2011.

Basu, S., Guerlet, S., Butz, A., Houweling, S., Hasekamp, O., Aben, I., Krummel, P., Steele, P., Langenfelds, R., Torn, M., Biraud, S., Stephens, B., Andrews, A., and Worthy, D.: Global CO_2 fluxes estimated from GOSAT retrievals of total column CO_2, Atmospheric Chemistry and Physics, 13, 8695–8717, doi:10.5194/acp-13-8695-2013, http://www.atmos-chem-phys.net/13/8695/2013/, 2013.

Bovensmann, H., Buchwitz, M., Burrows, J. P., Reuter, M., Krings, T., Gerilowski, K., Schneising, O., Heymann, J., Tretner, A., and Erzinger, J.: A remote sensing technique for global monitoring of power plant CO_2 emissions from space and related applications, Atmospheric Measurement Techniques Discussion, 3, 55–110, 2010.

Bureau of the Environment Tokyo: Tokyo Cap-and-Trade Program: Japan's first mandatory emissions trading scheme, Tech. rep., Tokyo Metropolitan Government, https://www.kankyo.metro.tokyo.jp/en/attachement/Tokyo-cap_and_trade_program-march_2010_TMG.pdf, 2010.

Butz, A., Dinger, A. S., Bobrowski, N., Kostinek, J., Fieber, L., Fischerkeller, C., Giuffrida, G. B., Hase, F., Klappenbach, F., Kuhn, J., Lübcke, P., Tirpitz, L., and Tu, Q.: Remote sensing of volcanic CO_2, HF, HCl, SO_2, and BrO in the downwind plume of Mt. Etna, Atmospheric Measurement Techniques Discussions, 2016, 1–26, doi:10.5194/amt-2016-254, http://www.atmos-meas-tech-discuss.net/amt-2016-254/, 2016.

Chen, J., Viatte, C., Hedelius, J. K., Jones, T., Franklin, J. E., Parker, H., Gottlieb, E. W., Wennberg, P. O., Dubey, M. K., and Wofsy, S. C.: Differential column measurements using compact solar-tracking spectrometers, Atmospheric Chemistry and Physics, 16, 8479–8498, doi:10.5194/acp-16-8479-2016, http://www.atmos-chem-phys.net/16/8479/2016/, 2016.

Collins, M., Knutti, R., Arblaster, J., Dufresne, J.-L., Fichefet, T., Friedlingstein, P., Gao, X., Gutowski, W., Johns, T., Krinner, G., Shongwe, M., Tebaldi, C., Weaver, A., and Wehner, M.: Long-term Climate Change: Projections, Commitments and Irreversibility, book section 12, p. 1029–1136, Cambridge University Press, Cambridge, United Kingdom and New York, NY, USA, doi:10.1017/CBO9781107415324.024, www.climatechange2013.org, 2013.

Deng, F., Jones, D. B. A., Henze, D. K., Bousserez, N., Bowman, K. W., Fisher, J. B., Nassar, R., O'Dell, C., Wunch, D., Wennberg, P. O., Kort, E. A., Wofsy, S. C., Blumenstock, T., Deutscher, N. M., Griffith, D. W. T., Hase, F., Heikkinen, P., Sherlock, V., Strong, K., Sussmann, R., and Warneke, T.: Inferring regional sources and sinks of atmospheric CO_2 from GOSAT XCO_2 data, Atmospheric Chemistry and Physics, 14, 3703–3727, doi:10.5194/acp-14-3703-2014, http://www.atmos-chem-phys.net/14/3703/2014/, 2014.

Frey, M., Hase, F., Blumenstock, T., Groß, J., Kiel, M., Mengistu Tsidu, G., Schäfer, K., Sha, M. K., and Orphal, J.: Calibration and instrumental line shape characterization of a set of portable FTIR spectrometers for detecting greenhouse gas emissions, Atmospheric Measurement Techniques, 8, 3047–3057, doi:10.5194/amt-8-3047-2015, https://www.atmos-meas-tech.net/8/3047/2015/, 2015.

Hakkarainen, J., Ialongo, I., and Tamminen, J.: Direct space-based observations of anthropogenic CO_2 emission areas from OCO-2, Geophysical Research Letters, pp. n/a–n/a, doi:10.1002/2016GL070885, 2016.

Hammerling, D. M., Michalak, A. M., and Kawa, S. R.: Mapping of CO_2 at high spatiotemporal resolution using satellite observations: Global distributions from OCO-2, Journal of Geophysical Research, 117, D06 306, doi:10.1029/2011JD017015, 2012.

Hartmann, D., Klein Tank, A., Rusticucci, M., Alexander, L., Brönnimann, S., Charabi, Y., Dentener, F., Dlugokencky, E., Easterling, D., Kaplan, A., Soden, B., Thorne, P., Wild, M., and Zhai, P.: Observations: Atmosphere and Surface, book section 2, p. 159–254, Cambridge University Press, Cambridge, United Kingdom and New York, NY, USA, doi:10.1017/CBO9781107415324.008, www.climatechange2013.org, 2013.

Hase, F., Frey, M., Blumenstock, T., Groß, J., Kiel, M., Kohlhepp, R., Mengistu Tsidu, G., Schäfer, K., Sha, M. K., and Orphal, J.: Application of portable FTIR spectrometers for detecting greenhouse gas emissions of the major city Berlin, Atmospheric Measurement Techniques, 8, 3059–3068, doi:10.5194/amt-8-3059-2015, http://www.atmos-meas-tech.net/8/3059/2015/, 2015.

Hunter, J.: Matplotlib: A 2D Graphics Environment, Computing in Science Engineering, 9, 90–95, doi:10.1109/MCSE.2007.55, 2007.

Ichii, K., Ueyama, M., Kondo, M., Saigusa, N., Kim, J., Alberto, M. C., Ardö, J., Euskirchen, E. S., Kang, M., Hirano, T., Joiner, J., Kobayashi, H., Belelli Marchesini, L., Merbold, L., Miyata, A., Saitoh, T. M., Takagi, K., Varlagin, A., Bret-Harte, M. S., Kitamura, K., Kosugi, Y., Kotani, A., Kumar, K., Li, S.-G., Machimura, T., Matsuura, Y., Mizoguchi, Y., Ohta, T., Mukherjee, S., Yanagi, Y., Yasuda, Y., Zhang, Y., and Zhao, F.: New data-driven estimation of terrestrial CO_2 fluxes in Asia using a standardized database of eddy covariance measurements, remote sensing data, and support vector regression, Journal of Geophysical Research: Biogeosciences, pp. n/a–n/a, doi:10.1002/2016JG003640, 2017.

Ijima, O.: Radiosonde measurements from station Tateno (2015-12), doi:10.1594/PANGAEA.858510, https://doi.pangaea.de/10.1594/PANGAEA.858510, 2016.

Klappenbach, F., Bertleff, M., Kostinek, J., Hase, F., Blumenstock, T., Agusti-Panareda, A., Razinger, M., and Butz, A.: Accurate mobile remote sensing of XCO_2 and XCH_4 latitudinal transects from aboard a research vessel, Atmospheric Measurement Techniques, 8, 5023–5038, doi:10.5194/amt-8-5023-2015, http://www.atmos-meas-tech.net/8/5023/2015/, 2015.

Kunreuther, H., Gupta, S., Bosetti, V., Cooke, R., Dutt, V., Ha-Duong, M., Held, H., Llanes-Regueiro, J., Patt, A., Shittu, E., and Weber, E.: Integrated Risk and Uncertainty Assessment of Climate Change Response Policies, chap. 2, pp. 151–206, Working Group III to the Fifth Assessment Report of the Intergovernmental Panel on Climate Change, 2014.

Le Quéré, C., Moriarty, R., Andrew, R. M., Peters, G. P., Ciais, P., Friedlingstein, P., Jones, S. D., Sitch, S., Tans, P., Arneth, A., Boden, T. A., Bopp, L., Bozec, Y., Canadell, J. G., Chini, L. P., Chevallier, F., Cosca, C. E., Harris, I., Hoppema, M., Houghton, R. A., House, J. I., Jain, A. K., Johannessen, T., Kato, E., Keeling, R. F., Kitidis, V., Klein Goldewijk, K., Koven, C., Landa, C. S., Landschützer, P., Lenton, A., Lima, I. D., Marland, G., Mathis, J. T., Metzl, N., Nojiri, Y., Olsen, A., Ono, T., Peng, S., Peters, W., Pfeil, B., Poulter, B., Raupach, M. R., Regnier, P., Rödenbeck, C., Saito, S., Salisbury, J. E., Schuster, U., Schwinger, J., Séférian, R., Segschneider, J., Steinhoff, T., Stocker,

B. D., Sutton, A. J., Takahashi, T., Tilbrook, B., van der Werf, G. R., Viovy, N., Wang, Y.-P., Wanninkhof, R., Wiltshire, A., and Zeng, N.: Global carbon budget 2014, Earth System Science Data, 7, 47–85, doi:10.5194/essd-7-47-2015, http://www.earth-syst-sci-data.net/7/47/2015/, 2015.

Le Quéré, C., Andrew, R. M., Canadell, J. G., Sitch, S., Korsbakken, J. I., Peters, G. P., Manning, A. C., Boden, T. A., Tans, P. P., Houghton, R. A., Keeling, R. F., Alin, S., Andrews, O. D., Anthoni, P., Barbero, L., Bopp, L., Chevallier, F., Chini, L. P., Ciais, P., Currie, K., Delire, C., Doney, S. C., Friedlingstein, P., Gkritzalis, T., Harris, I., Hauck, J., Haverd, V., Hoppema, M., Klein Goldewijk, K., Jain, A. K., Kato, E., Körtzinger, A., Landschützer, P., Lefèvre, N., Lenton, A., Lienert, S., Lombardozzi, D., Melton, J. R., Metzl, N., Millero, F., Monteiro, P. M. S., Munro, D. R., Nabel, J. E. M. S., Nakaoka, S.-I., O'Brien, K., Olsen, A., Omar, A. M., Ono, T., Pierrot, D., Poulter, B., Rödenbeck, C., Salisbury, J., Schuster, U., Schwinger, J., Séférian, R., Skjelvan, I., Stocker, B. D., Sutton, A. J., Takahashi, T., Tian, H., Tilbrook, B., van der Laan-Luijkx, I. T., van der Werf, G. R., Viovy, N., Walker, A. P., Wiltshire, A. J., and Zaehle, S.: Global Carbon Budget 2016, Earth System Science Data, 8, 605–649, doi:10.5194/essd-8-605-2016, http://www.earth-syst-sci-data.net/8/605/2016/, 2016.

Massart, S., Agusti-Panareda, A., Aben, I., Butz, A., Chevallier, F., Crevosier, C., Engelen, R., Frankenberg, C., and Hasekamp, O.: Assimilation of atmospheric methane products in the MACC-II system: from SCIAMACHY to TANSO and IASI, Atmospheric Chemistry and Physics Discussions, 14, 2553–2599, doi:10.5194/acpd-14-2553-2014, 2014.

Meesters, A. G. C. A., Tolk, L. F., Peters, W., Hutjes, R. W. A., Vellinga, O. S., Elbers, J. A., Vermeulen, A. T., van der Laan, S., Neubert, R. E. M., Meijer, H. A. J., and Dolman, A. J.: Inverse carbon dioxide flux estimates for the Netherlands, Journal of Geophysical Research: Atmospheres, 117, doi:10.1029/2012JD017797, 2012.

Messerschmidt, J., Geibel, M. C., Blumenstock, T., Chen, H., Deutscher, N. M., Engel, A., Feist, D. G., Gerbig, C., Gisi, M., Hase, F., Katrynski, K., Kolle, O., Lavrič, J. V., Notholt, J., Palm, M., Ramonet, M., Rettinger, M., Schmidt, M., Sussmann, R., Toon, G. C., Truong, F., Warneke, T., Wennberg, P. O., Wunch, D., and Xueref-Remy, I.: Calibration of TCCON column-averaged CO_2: the first aircraft campaign over European TCCON sites, Atmospheric Chemistry and Physics, 11, 10 765–10 777, doi:10.5194/acp-11-10765-2011, http://www.atmos-chem-phys.net/11/10765/2011/, 2011.

Morino, I., Matsuzaki, T., and Horikawa, M.: TCCON data from Tsukuba (JP), 125HR, Release GGG2014.R1, TCCON data archive, hosted by CaltechData, doi:10.14291/tccon.ggg2014.tsukuba02.R1/1241486, 2016.

Nassar, R., Napier-Linton, L., Gurney, K. R., Andres, R. J., Oda, T., Vogel, F. R., and Deng, F.: Improving the temporal and spatial distribution of CO2 emissions from global fossil fuel emission data sets, Journal of Geophysical Research: Atmospheres, 118, 917–933, doi:10.1029/2012JD018196, https://agupubs.onlinelibrary.wiley.com/doi/abs/10.1029/2012JD018196, 2013.

Oda, T. and Maksyutov, S.: A very high-resolution (1 km×1 km) global fossil fuel CO_2 emission inventory derived using a point source database and satellite observations of nighttime lights, Atmospheric Chemistry and Physics, 11, 543–556, doi:10.5194/acp-11-543-2011, http://www.atmos-chem-phys.net/11/543/2011/, 2011.

Ohyama, H., Morino, I., Nagahama, T., Machida, T., Suto, H., Oguma, H., Sawa, Y., Matsueda, H., Sugimoto, N., Nakane, H., and Nakagawa, K.: Column-averaged volume mixing ratio of CO_2 measured with ground-based Fourier transform spectrometer at Tsukuba, Journal of Geophysical Research: Atmospheres, 114, n/a–n/a, doi:10.1029/2008JD011465, http://dx.doi.org/10.1029/2008JD011465, d18303, 2009.

Peters, W. and van der Laan-Luijkx, I.: Fossil Fuel Prior Fluxes compiled for the GEOCARBON project, 2012.

Riddick, S. N., Connors, S., Robinson, A. D., Manning, A. J., Jones, P. S. D., Lowry, D., Nisbet, E., Skelton, R. L., Allen, G., Pitt, J., and Harris, N. R. P.: Estimating the size of a methane emission point source at different scales: from local to landscape, Atmospheric Chemistry and Physics, 17, 7839–7851, doi:10.5194/acp-17-7839-2017, https://www.atmos-chem-phys.net/17/7839/2017/, 2017.

Atmospheric Measurement Techniques Discussions

Rolph, G., Stein, A., and Stunder, B.: Real-time Environmental Applications and Display sYstem: {READY}, Environmental Modelling & Software, 95, 210 – 228, doi:https://doi.org/10.1016/j.envsoft.2017.06.025, http://www.sciencedirect.com/science/article/pii/S1364815217302360, 2017.

secretariat, U.: The Paris Agreement, unfccc.int/paris_agreement/items/9485.php, last accessed: 2017-09-18, 2015.

Stein, A. F., Draxler, R. R., Rolph, G. D., Stunder, B. J. B., Cohen, M. D., and Ngan, F.: NOAA's HYSPLIT Atmospheric Transport and Dispersion Modeling System, Bulletin of the American Meteorological Society, 96, 2059–2077, doi:10.1175/BAMS-D-14-00110.1, https://doi.org/10.1175/BAMS-D-14-00110.1, 2015.

Toon, G., Blavier, J.-F., Washenfelder, R., Wunch, D., Keppel-Aleks, G., Wennberg, P., Connor, B., Sherlock, V., Griffith, D., Deutscher, N., and Notholt, J.: Total Column Carbon Observing Network (TCCON), in: Advances in Imaging, p. JMA3, Optical Society of America, doi:10.1364/FTS.2009.JMA3, http://www.opticsinfobase.org/abstract.cfm?URI=FTS-2009-JMA3, 2009.

van der Laan-Luijkx, I. T., van der Velde, I. R., van der Veen, E., Tsuruta, A., Stanislawska, K., Babenhauserheide, A., Zhang, H. F., Liu, Y., He, W., Chen, H., Masarie, K. A., Krol, M. C., and Peters, W.: The CarbonTracker Data Assimilation Shell (CTDAS) v1.0: implementation and global carbon balance 2001–2015, Geoscientific Model Development Discussions, 2017, 1–30, doi:10.5194/gmd-2017-45, http://www.geosci-model-dev-discuss.net/gmd-2017-45/, 2017.

van der Velde, I. R., Miller, J. B., Schaefer, K., van der Werf, G. R., Krol, M. C., and Peters, W.: Terrestrial cycling of $^{13}CO_2$ by photosynthesis, respiration, and biomass burning in SiBCASA, Biogeosciences, 11, 6553–6571, doi:10.5194/bg-11-6553-2014, http://www.biogeosciences.net/11/6553/2014/, 2014a.

van der Velde, I. R., Miller, J. B., Schaefer, K., van der Werf, G. R., Krol, M. C., and Peters, W.: Towards multi-tracer data-assimilation: biomass burning and carbon isotope exchange in SiBCASA, Biogeosciences Discussions, 11, 107–149, doi:10.5194/bgd-11-107-2014, http://www.biogeosciences-discuss.net/11/107/2014/, 2014b.

Wunch, D., Toon, G. C., Blavier, J.-F. L., Washenfelder, R., Notholt, J., Connor, B. J., Griffith, D. W. T., Sherlock, V., and Wennberg, P. O. W.: The Total Carbon Column Observing Network, Phil. Trans. R. Soc. A, 369, doi:10.1098/rsta.2010.0240, 2011.